Polymer 49 (2008) 4949–4959

Contents lists available at ScienceDirect

Polymer

journal homepage: www.elsevier.com/locate/polymer

Structure–property relationships for a series of polyimide copolymers with sulfonated pendant groups

Olivier Savard [a,1], Timothy J. Peckham [a,b], Yunsong Yang [a,2], Steven Holdcroft [a,b,*]

[a] Department of Chemistry, Simon Fraser University, Burnaby, British Columbia V5A 1S6, Canada
[b] Institute for Fuel Cell Innovation, National Research Council Canada, 4250 Wesbrook Mall, Vancouver, British Columbia V6T 1W5, Canada

ARTICLE INFO

Article history:
Received 29 July 2008
Received in revised form 3 September 2008
Accepted 5 September 2008
Available online 20 September 2008

Keywords:
Polyimide
Proton exchange membrane
Structure–property relationships

ABSTRACT

A series of high molecular weight, sulfonated polyimide copolymers (**8a–f**) with controlled acid contents have been obtained using 2,2′-bis(4-sulfobenzyloxy)benzidine (**14**) prepared via a flexible synthetic route. This series of novel sulfonated polyimide membranes were found to possess higher hydrolytic stability than polyimides in which the sulfonic acid groups are bound directly to the polymer main chain. An in-depth analysis of conductivity data was also performed for **8** and compared to the results for Nafion® (**1**), sulfonated poly(ether ether ketone) (**2**) and a main-chain sulfonated polyimide (**3**). In order to remove the influence of acid strength, the proton mobility value for **8** at infinite dilution was calculated and found to be $1.2(\pm 0.6) \times 10^{-3}$ cm^2 s^{-1} V^{-1}. A catalyst-coated membrane (CCM)-MEA based on a polyimide incorporating 60% sulfonated monomer (**8d**) was found to exhibit comparable beginning-of-life fuel cell performance as a Nafion®-based CCM MEA at 50 °C.

1. Introduction

The proton exchange membrane (PEM) has a number of roles in a PEM fuel cell (PEMFC), including separation of reactant gases, transportation of protons from anode to cathode and providing an environment for electrode reactions to occur at the electrolyte/electrode interfaces. In order to be suitable for PEMFC applications, a membrane ideally possesses a variety of different characteristics such as low cost, high proton conductivity, low permeability to fuel and oxidant, low electrical conductivity, balanced water transport, oxidative and hydrolytic stabilities, good mechanical properties and capability to be assembled into a membrane electrode assembly (MEA) [1,2]. Furthermore, for PEMFC-based applications to achieve commercial success, the membrane must be capable of performing well under increasingly stringent operating conditions (e.g., high temperature, low relative humidity) [2,3]. Even Nafion® (**1**), currently the most widely used membrane, does not satisfactorily meet all of these criteria (Fig. 1).

A variety of different polymer systems (e.g., perfluorinated and partially fluorinated ionomers, polystyrene-based systems, sulfonated polyarylenes) have been investigated for their suitability as PEMs [2,4–9]. Sulfonated polyarylene-based systems (e.g., sulfonated poly(ether ether ketone), SPEEK, **2**) are one of the most widely studied due to the attractive mechanical properties, as well as thermal and chemical stabilities of the parent, high temperature, thermoplastics [2]. Examples of polyarylene-based systems that have been studied for application as PEMs include poly(phenylene)s [10–16], poly(arylene ether)s [2,17], poly(arylene ether sulfides) [2,18,19], polyimides [20–23] and polybenzimidazoles [24–27]. In addition to the previously mentioned advantages, polyarylenes are relatively easily to functionalize and can be readily sulfonated by reagents such as concentrated sulphuric acid, fuming sulphuric acid, chlorosulfonic acid and sulphur trioxide. However, post-sulfonation reactions suffer from a lack of control over the degree and location of functionalization, in addition to potential side reactions (e.g., cross-linking) and/or degradation of the polymer backbone [28,29]. More recently, improvements in this area have been achieved by the use of sulfonated monomers which allow both for control over the degree of sulfonation as well as preventing the occurrence of side reactions or degradation [18,30–36]. Direct polymerization of sulfonated monomers also provides the possibility of polymer microstructure design, such as block or graft copolymers, which have been demonstrated to exhibit advantages over random copolymers for fuel cell application [19,37–46].

Due to their excellent thermal, chemical and mechanical stabilities, relatively facile synthesis of high molecular weight polymer, readily available commercial starting materials, and resistance to swelling, sulfonated polyimides (e.g., **3**) are attractive

* Corresponding author. Department of Chemistry, Simon Fraser University, 8888 University Drive, Burnaby, British Columbia V5A 1S6, Canada.
E-mail address: holdcrof@sfu.ca (S. Holdcroft).
[1] Present address: PerkinElmer LAS Canada Inc., 501 Rowntree Dairy Road, Unit #6 Woodbridge, Ontario L4L 8H1, Canada.
[2] Present address: Ballard Power Systems, 9000 Glenlyon Parkway, Burnaby, British Columbia V5J 5J9, Canada.

0032-3861/$ – see front matter © 2008 Elsevier Ltd. All rights reserved.
doi:10.1016/j.polymer.2008.09.011

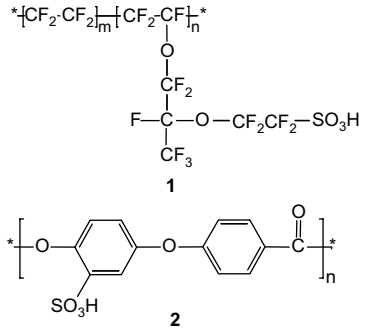

Fig. 1. Archetypal polymers used in PEMs: Nafion® (**1**) and SPEEK (**2**).

materials for application as membranes in PEMFCs [23]. Studies on sulfonated polyimides have found that phthalic-based systems readily degrade due to hydrolysis of the carbonyl carbon–nitrogen bond whereas naphthalic-based sulfonated polyimides (**3**) are significantly more stable [47,48]. Thus, most of the research on sulfonated polyimide as PEMs have focussed on naphthalic-based systems [20–23,48–59].

Although polyimide-based systems have been developed with the sulfonic acid groups directly bound to the polymer backbone, Okamoto et al. [49–54] (**4**) and Watanabe et al. [55,56,59] (**5**) have recently reported the synthesis of sulfonated polyimides in which the sulfonic acid groups are separated from the polymer main chain via an alkyl ether spacer unit. This has led to greater hydrolytic stability over those polyimides in which the sulfonic acid groups are directly bound to the polymer backbone. It has been shown that the hydrolytic stability of polyimides is dependent on the basicity of the amido nitrogen; the greater its basicity, the greater the stability of the carbonyl carbon–nitrogen bond against hydrolysis [60]. The strong electron-withdrawing effect of the sulfonic acid group decreases the electron density in the phenyl ring and thus also the basicity of the neighbouring nitrogen centre. This effect of the sulfonic acid group is decreased if a spacer group is placed between the $-SO_3H$ group and the phenyl ring, thereby increasing relative hydrolytic stability. In the case of **4** and **5**, the electron-donating ethereal oxygen further increases the basicity of the nitrogen centre and hydrolytic stability.

To synthesize **4**, Okamoto et al. employed a rearrangement reaction to synthesize the side-chain sulfonated benzidine monomer [49,50,52–54]. This route, however, is not particularly flexible and only a limited number of different chemical structures can be made. Watanabe et al. used sultone ring-opening reactions to obtain suitable monomers to synthesize **5** but, given the generally difficulty in synthesizing sultone rings and the restriction of this method to only strained rings, this route is also limited in scope [55]. More recently, Watanabe et al. used a relatively flexible route to produce acetamido-protected (for the amine functionalities) sulfonated benzidine monomers bearing long (*n*-$C_{10}H_{21}$ or *n*-$C_{12}H_{25}$), aliphatic side chains that were subsequently polymerized in order to yield **6e–f** with fluorenyl moieties in the main chain [56]. Hydrolytic stability was found to increase as a function of side-chain length where the polymers with shorter side-chain length, **6a–d** displayed lower stability than those with longer side-chain lengths, **6f** having the greatest stability within this series of polymers. However, proton conductivity values were found to be lower for the long side-chain sulfonated polymers, presumably due to their relatively lower IEC values.

Our group has also been actively investigating polyimides as model systems for exploring structure–property relationships of PEMs [57,58]. In our initial study, the effects of introducing angled moieties into the polymer backbone (**7**) were examined. It was found that linear polyimides (**3**) possessed lower conductivity values for a given ion exchange capacity (IEC) value. This was shown to be due to higher water content for the linear polymer, thereby leading to lower proton concentrations, whereas proton mobility values were found to be relatively similar. It was theorized that the angled monomer led to greater number of chain entanglements and thus a greater resistance to swelling [57].

As part of our continued interest in structure–property relationships for polyimides, we report our work on polyimides with sulfonated side chains (**8**) [58]. In this paper, we provide details on an improved synthetic route to 2,2′-bis(4-sulfobenzyloxy)benzidine-based monomers (**14**), thereby providing easier access to a wide variety of different sulfonated side-chain polyimides suitable for an extensive study on polyimide-based PEM structure–property relationships (Fig. 2). Furthermore, we report the synthesis and characterization of copolymers (**8a–f**) incorporating this monomer wherein ion content was controlled by altering the monomer feed ratios, and the results of beginning-of-life fuel cell tests.

2. Experimental

2.1. Materials and methods

Unless otherwise mentioned, all reagents were purchased from Sigma–Aldrich, Canada and were used as-received. Compound **12** (4-bromomethyl-benzenesulfonic acid, sodium salt) was synthesized according to a literature procedure [62].

2.2. Synthesis of 2,2′-bis(4-sulfobenzyloxy)benzidine (*14*)

To a suspension of 3,3′-dihydroxybenzidine (**9**) (1.000 g, 4.625 mmol) in 30 mL of anhydrous ethanol was added

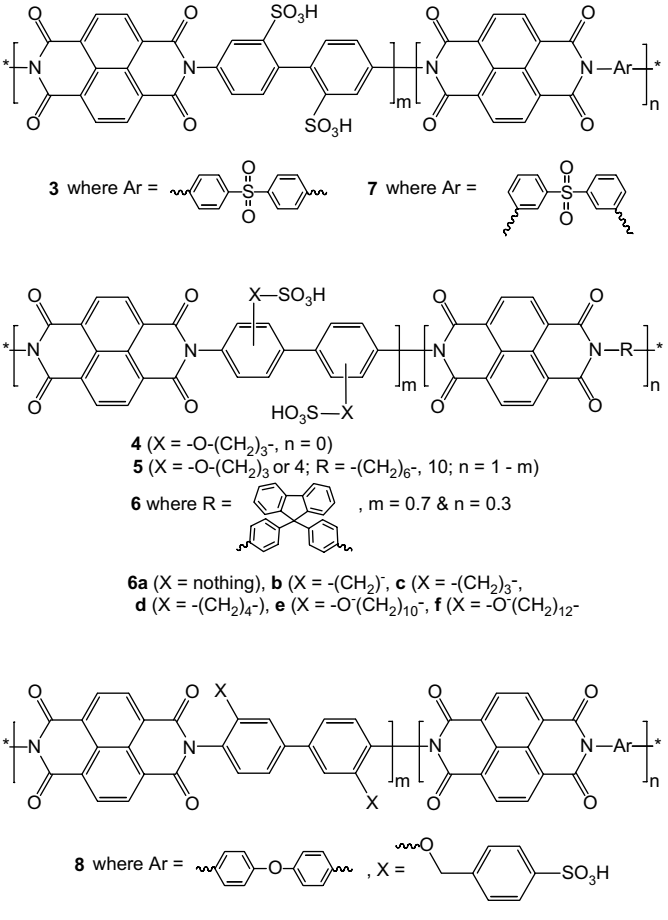

Fig. 2. Examples of potential sulfonated polyimide-based PEMs [53–59,61].

benzophenone imine (**10**) (1.7604 g, 9.713 mmol). The suspension was refluxed overnight. The light brown suspension turned bright yellow after 5 h. The suspension was then filtered and washed with methanol to give the pure bright yellow compound *N*,*N*′-bis(diphenylmethylene)-*o*-aminophenol (**11**). Yield: 2.12 g (88%). ^{1}H NMR (DMSO-d_6, 500 MHz) δ 9.07 (1H, s), 7.64 (2H, d, 7.0 Hz), 7.51 (1H, t), 7.44 (3H, m), 7.29 (2H, t, 8.0 Hz), 7.16 (2H, d, 7.5 Hz), 6.85 (1H, s), 6.68 (1H, d, 8 Hz), 6.37 (1H, d, 8 Hz). ^{13}C NMR (DMSO-d_6, 100 MHz) δ 168.19, 147.87, 138.97, 138.42, 136.49, 135.44, 130.78, 128.23, 120.69, 116.36, 112.75. FTIR (KBr cm^{-1}): 3200 (O–H stretch), 3050 (Ar–H stretch), 1588 (C=C stretch), 1560 (C=N stretch), 1480 (C=C stretch), 1323 (C–N stretch), 1188 (C–O stretch). Calcd. for $C_{38}H_{28}O_2N_2$: C 83.80; H 5.18; N 5.14. Found: C 83.55; H 5.39; N 4.91.

To a suspension of **11** (1.0000 g, 1.921 mmol) and **12** (1.0129 g, 4.034 mmol) in DMF was added sodium hydride (0.0968 g, 4.03 mmol). The reaction was left stirring overnight under nitrogen at room temperature. The yellow suspension turned instantly red after adding NaH and became soluble after 2 h, with a red precipitate forming after approximately 5 h. Methanol was added to the solution and the white precipitate filtered and washed with methanol to give **13**. Compound **13** was acidified with 2 M HCl for 24 h to remove the protecting groups. The remaining solid was filtered and rinsed with Millipore water. The intermediate was then solubilized in 1 M NaOH. The reddish solution was then filtered to remove the insoluble products. The filtrate was then poured in 2 M HCl and gives a light brown precipitate. The precipitate was then isolated by centrifugation and dried under vacuum at 80 °C overnight. The dry product was washed with chloroform to give 2,2′-bis(4-sulfobenzyloxy)benzidine (**14**). Yield: 0.89 g (83%). ^{1}H NMR (DMSO-d_6, 500 MHz): δ 7.61 (2H, d, 8.0 Hz), 7.47 (2H, d, 8.0 Hz), 7.06 (1H, d), 6.89 (1H, dd, 8.5 Hz), 6.66 (1H, d, 8 Hz), 5.14 (2H, s), 4.68 (2H, s). ^{13}C NMR (DMSO-d_6, 100 MHz): δ 152.97, 150.79, 142.99, 141.52, 134.74, 132.03, 130.77, 123.80, 119.57, 115.35, 74.47. FTIR (KBr cm^{-1}): 3405–2621 (NH_3 stretch), 3050 (Ar–H stretch), 2919 (C–H stretch), 1628 (N–H rocking), 1502 (C=C stretch), 1398 (N–H rocking), 1270 (C–N stretch), 1238 (S=O asym. stretch), 1123 (S=O sym. stretch), 1030 (C–O stretch). Calcd. for $C_{26}H_{24}O_8N_2S_2$: C 56.10; H 4.35; N 5.03. Found: C 55.89; H 4.54; N 4.90.

2.3. Synthesis of sulfonated side-chain polyimides (*8a–f*) using *8d* as example

To a dry, three necked flask equipped with a Dean Stark trap and condenser were added 2,2′-bis(4-sulfobenzyloxy)benzidine (**14**) (0.2783 g, 0.5000 mmol), 4,4′-oxybisbenzenamine (**15**) (0.06674 g, 0.3333 mmol) and 1,4,5,8-naphthalenetetracarboxylic dianhydride (**16**) (0.2235 g, 0.8333 mmol) under nitrogen. To this was added *m*-cresol (5 mL), chlorobenzene (7 mL) and triethylamine (0.1214 g, 1.200 mmol). The mixture was stirred for 2–3 h until complete dissolution of the monomers occurred. Benzoic acid (0.1221 g, 1.000 mmol) was then added to the solution and the temperature increased to 150 °C for 2 h. Chlorobenzene was then removed from the solution and the temperature was brought to 180 °C for 24 h. After a few hours, the solution viscosity was observed to increase. Upon cooling down the solution, additional *m*-cresol (10 mL) was added to dilute the reaction mixture. The polymer was then precipitated into MeOH. After filtration, remaining *m*-cresol was removed using a Soxhlet extractor with MeOH as solvent for 48 h. The polymer was then dried under vacuum at 80 °C for 24 h. Yield: 0.53 g (99%). ^{1}H NMR (DMSO-d_6, 500 MHz): δ 8.78 (br), 7.77 (br), 7.56 (br), 7.49 (br), 7.39–7.22 (br), 5.28 (br). FTIR (drop cast on NaCl, cm^{-1}): 3442 (H_2O/O–H stretch), 3074–3007 (Ar–H stretch), 2915 (C–H stretch), 1715 (C=O sym. stretch), 1675 (C=O asym. stretch), 1582 (C=C stretch), 1499 (C=C stretch), 1448 (C=C stretch), 1349 (C–N stretch), 1251 (Ar–O stretch), 1199 (C–O stretch), 1123 (S=O stretch), 1037 (SO_3 sym. stretch), 1012 (S–OH stretch). *Membrane casting*: the polymer was dissolved in DMSO after which the viscous solution was then filtered, cast onto a flat, glass petri dish and dried at 80 °C for 24 h. *Note*: Other copolymers in the series were synthesized using the same method by changing the molar feed ratio of **14**:**15** in order to obtain copolymers with different IEC values.

2.4. Instrumentation

^{1}H NMR spectra were obtained on a Varian Unity Spectrometer 500 MHz operating at 500 MHz and ^{13}C NMR spectra from a Bruker Unity Spectrometer 400 MHz operating at 100.4 MHz. The compounds were dissolved in DMSO-d_6 at a concentration of ~10 mg/mL. Triethylamine was added to the sulfonated monomer solution to increase its solubility. For the sulfonated polyimides, the salt form ($SO_3^-(CH_3CH_2)_3NH^+$) was used due to its higher solubility compared to the acid form. Fourier transform infrared spectroscopy (FTIR) was performed on a Bomem FTLA2000-154 FTIR system. For the sulfonated monomer and its intermediate, KBr pellets were made with the appropriate compound. Sulfonated polyimides (sodium form) were drop cast from a DMSO solution on a NaCl window and dried under vacuum at 80 °C for 2 h prior to measurements. Elemental analysis was used to determine the composition of the sulfonated monomer (**14**) and its intermediate (**13**), using a Carlo Erba model 1106 CHN analyzer. Thermogravimetric analysis (TGA) was performed on the sulfonated polyimides (acid form) on a 2950 TGA HR instrument at a rate of 10 °C/min under nitrogen from 50 to 550 °C. Prior to measurement, the samples were dried at 150 °C for 30 min in the instrument chamber to remove excess water. The measurements of reduced and inherent viscosities of synthesized sulfonated polyimides were performed using a homemade viscometer, thermally controlled by a circulating water system. An automatic timer, controlled by a refractive index detector, was used to make the time measurements. Viscosities were measured at 30 °C in *m*-cresol. Viscosity provides information on the size of a polymer molecule in solution.

2.5. Membrane water weight uptake (WU)

After casting, membranes were soaked in 2 M HCl for 48 h, then rinsed and soaked for 2 h at room temperature in Millipore H_2O. The membranes were dried in a vacuum oven at 80 °C for 24 h. The dry membranes were then weighed, soaked again in Millipore H_2O for 48 h, and weighed again. Water uptake is reported as a percentage uptake and determined by taking the equilibrium weight difference between the wet film (W_{wet}) and the dry film (W_{dry}) and dividing by the dry film (W_{dry}) weight. The equation is given below:

$$\text{Water uptake} = \frac{w_{wet} - w_{dry}}{w_{dry}} \times 100 \quad (1)$$

To obtain the value of water uptake of a membrane, the average water uptake of three membranes with the same theoretical ion exchange capacity was measured.

2.6. Membrane water volume uptake (VU)

The acidified membranes were first immersed in Millipore water for 24 h at room temperature. Membrane thickness was then measured with Series 293 Mitutoyo Quickmike Series calipers while length and width were measured with Series 500 Mitutoyo Digimatic Calipers. The membranes were dried under vacuum at 80 °C overnight and the dry volume was measured. VU was calculated using Eq. (2):

$$\text{Volume uptake} = \frac{V_{wet} - V_{dry}}{V_{dry}} \times 100 \quad (2)$$

2.7. Membrane water volume fraction (X_v)

The membrane water volume fraction was calculated according to the following equation:

$$X_v = \frac{V_{water}}{V_{wet}} \tag{3}$$

where $V_{wet} = (w_{wet} - w_{dry})/\rho_{wet}$.

2.8. Ion exchange capacity from titration (IEC_{Titr})

Copolymers (**8a–f**) in the acid form were dried overnight at 80 °C under vacuum, weighed and then immersed in 2 N NaCl for 1 h. Titrations were carried out using 2 N NaOH as titrant (standardized against dry potassium biphthalate) and phenolphthalein as indicator. The reported experimentally determined ion exchange capacities are the average of at least three separate titrated samples. Eq. (4) was used to calculate the ion exchange capacity. The volume of NaOH used to reach the end point (V_{NaOH}), the concentration of the NaOH solution used ([NaOH]) and the dry weight of the membrane ($w_{membrane}$) were needed to calculate the ion exchange capacity.

$$IEC = \frac{V_{NaOH} - [NaOH]}{w_{membrane}} \times 100 \tag{4}$$

2.9. Ion exchange capacity from ^1H NMR (IEC_{NMR})

^1H NMR was used to confirm the polymer structure and to measure the ion exchange capacity (IEC_{NMR}) and compare the results with the titration method (IEC_{Titr}). To determine IEC, the ratio between the benzylic protons (only present in the sulfonated monomer unit, SM) and the aromatic protons (present in SM and other monomer units (M)) was measured. This ratio, based on the molar feed ratio ($Ratio_{FR}$), was compared with the ratio obtained from the peak integration in ^1H NMR spectra ($Ratio_{NMR}$). Eq. (5) was used to calculate the aromatic/aliphatic protons ratio from the molar feed ratio. The number of aromatic protons in the sulfonated part ($H(SM_{Aromatic})$), in the non-sulfonated part ($H(M_{Aromatic})$) and the aliphatic proton ($H(SM_{Aliphatic})$) was also used:

$$\begin{aligned} Ratio &= \frac{H_{Aromatic}}{H_{Aliphatic}} \\ &= \frac{(H(SM_{Aromatic})) \times (x) + (H(M_{Aromatic})) \times (1-x)}{H\left(SM_{Aliphatic}\right)} \end{aligned} \tag{5}$$

The ion exchange capacity from NMR (IEC_{NMR}) was obtained using Eq. (6). The aromatic/aliphatic proton ratio obtained from NMR ($Ratio_{NMR}$) and molar feed ratio was first calculated.

$$IEC_{NMR} = \frac{IEC_{FR} \times Ratio_{NMR}}{Ratio_{FR}} \tag{6}$$

2.10. Lambda (λ)

This value represents the average number of H_2O molecules per sulfonic acid group. These were calculated using water uptake (WU) and IEC_{Titr} using Eq. (7):

$$\lambda = \frac{(WU/100)MW_{H_2O}}{IEC_{Titr} \times 1000^{-1}} \tag{7}$$

2.11. Proton conductivity

Proton conductivity was measured using AC impedance spectroscopy with a Solartron 1260 frequency response analyzer (FRA) employing a transverse two-electrode configuration. Rectangular samples ($\sim 1 \times 2$ cm) of membranes were cut to the required dimensions (length, L, and width, W, measured using a caliper, ±0.1 mm, and thickness, h, using a micrometer, ±0.001 mm). Samples were laid across two Pt electrodes (0.5×1 cm) 1 cm apart fixed in place by attaching to an inert 2 cm × 2 cm Teflon block (see Supplementary data). Another Teflon block was placed on top and four nylon screws were used to hold the probe together during measurement. Both blocks have identical 1×1 cm holes cut out of the centre to allow for membrane equilibration with the atmosphere where necessary. Membrane equilibration with water vapours of known relative humidity (±1.5% RH) was obtained at 25 °C (±0.1 °C) by placing the entire Pt/Teflon probe assembly into a computer controlled environmental test chamber. Temperature and relative humidity conditions were confirmed using an independently operated humidity sensor and digital thermometer.

Two wires fitted with alligator clips connected the probe to the frequency response analyzer and ionic resistance was measured by applying a 100 mV sinusoidal AC voltage between the two platinum electrodes over 10 MHz–100 Hz frequency range and measuring the AC resistance (i.e., impedance). Measurements were collected every half an hour during equilibration until constant ionic resistance was obtained. Data was analyzed using Zplot software (Scribner).

Ionic resistance was abstracted from the impedance data and fitting was performed by non-linear least squares regression to a standard Randles equivalent circuit model. In essence, the data can be approximated by taking the difference between the high frequency and low frequency x-intercepts, i.e., semi-circle diameter. The ionic resistance was used to calculate proton conductivity, σ_{H^+}, according to the following relationship (Eq. (8)):

$$\sigma_{H^+} = \frac{L}{R_m A} \tag{8}$$

where L is the spacing between the Pt electrodes (1.0 cm), A is the cross-sectional area of the membrane ($W \times h$), and R_m is the ionic resistance of the membrane.

2.12. Acid concentration ([–SO_3H]) and effective proton mobility (μ_{H^+})

Acid concentration for the membranes was determined according to Eq. (9):

$$[-SO_3H] = \frac{IEC \times w_{dry}}{V_{wet}} \tag{9}$$

where IEC is based on titration measurements.

The effective proton mobility was then calculated from Eq. (10):

$$\mu_{H^+} = \frac{\sigma_{H^+}}{F[-SO_3H]} \tag{10}$$

where F is Faraday's constant.

2.13. Membrane stability

The hydrolytic stability of the sulfonated polyimide membranes were determined by immersing the membranes into distilled water at 80 °C and characterized by the visible loss of mechanical strength. The mechanical stability test was made every 20 min for the first hour, every hour for 5 h and once a day until they lost their mechanical property as judged by their response to bending. The same test was simultaneously performed on the other membranes. An example of the test is provided in Supplementary data.

2.14. Fuel cell testing

Two different methods were used to prepare membrane electrode assemblies (MEAs): the catalyst-coated gas diffusion layer (CCGDL) and catalyst-coated membrane (CCM) methods. The CCGDL method consisted of coating Toray carbon paper 10%, wet-proofed (TGP-H60, PEMEAS, E-TEK Division) with a catalyst layer spray deposited from a heterogeneous mixture of 0.40 mg/cm^2 20% Pt/C (Vulcan XC-72, PEMEAS, E-TEK Division) with 30 wt% Nafion® (Sigma–Aldrich Co.) ionomer in aqueous solution of isopropanol. Copolymer **8d** (thickness = 30 μm) was hot pressed between these two CCGDLs at 135 °C for 90 s with approximately 90 kg cm^{-2} (~1280 psi) of pressure.

In the CCM method, a similar aqueous isopropanol based ink slurry having the composition 0.4 mg/cm^2 carbon supported 20% Pt/C (Vulcan XC-72, PEMEAS, E-TEK Division) and 30 wt% Nafion® ionomer content was spray deposited directly onto both sides of **8d** (thickness = 30 μm). To avoid overcompression of this deposited catalyst layer, the CCM was laminated with a ~35 μm thick polyethylene film exposing the active 5 cm^2 area at 80 °C through a rolling laminator. The CCM was sandwiched between two gas diffusion layers, SGL BC24 Gas Diffusion Media (GDM) (SGL Carbon Group) having a microporous layer (MPL). The MEA was assembled in the cell without hot pressing. A 125 μm thick compressible Si-gasket was used to assemble the gas diffusion media and to avoid gas leak within the cell. For Nafion®-based CCGDL and CCM anologues, N115 (thickness 138 μm) and N112 (thickness 55 μm) were used, respectively, with identical catalyst layers and GDMs as used for **8d**.

A triple serpentine 5 cm^2 single cell (Teledyne Energy Systems) was used for collecting fuel cell polarization data. The cell was operated with 200 mL/min of H_2 and O_2 at the anode and cathode at ambient pressure, respectively. Fully humidified reactant gases at 50 °C were supplied in a co-flow manner. The cell temperature was set at 50 °C. Polarization curves were obtained by reducing the potential from open circuit voltage (OCV) to 0.2 V in 50 mV increments and holding for 30 s at each point of the controlled potentials. Eight polarization curves were obtained in the same manner to confirm the polarization behaviour of the sample.

3. Results and discussion

3.1. Monomer synthesis

The synthesis of **14** (Fig. 3) was carried out by first protecting the amine functionalities as benzophenone imine groups [63]. The side chain reagent **12** was attached to *N*,*N*′-bis(diphenylmethylene)-*o*-aminophenol **11** via an S_N2 reaction and the amines subsequently deprotected via hydrolysis [64].

In the first step of the reaction, the amine groups of **9** were protected to yield **11**. By ^{1}H NMR spectroscopy, the amine peak of **9** (4.51 ppm) was observed to disappear whereas the hydroxyl group remained (singlet at 9.07 ppm). The hydroxyl peak was further identified by the addition of D_2O to the NMR solution whereby the fast exchange of D for H resulted in the disappearance of the hydroxyl peak. Additional spectroscopic evidence for the structure of **11** was found in the FTIR spectrum (O–H broad peak at 3200 cm^{-1}, peaks due to C=N at 1560 and 1323 cm^{-1}). Elemental analysis was also consistent with the molecular formula of **11**.

The second step of the synthesis consisted of the attachment of the sulfonated side chain (**12**) via the protected amine (**11**). Evidence for the reaction was the colour change (yellow to red) and the formation of bubbles (H_2) during the reaction. Deprotection was achieved via hydrolyzation of the imine group and isolation of **14** by precipitation of the salt intermediate (**13**) into 2 M HCl, thus converting it into its acid form. Excess **12** was removed by multiple washings, together with the by-product, benzophenone. Analyses of **14** by ^{1}H and ^{13}C NMR spectroscopies as well as FTIR (S=O stretching at 1238 and 1123 cm^{-1} and N–H stretching between 2621 and 3405 cm^{-1}) and elemental analysis were consistent with the assigned structure.

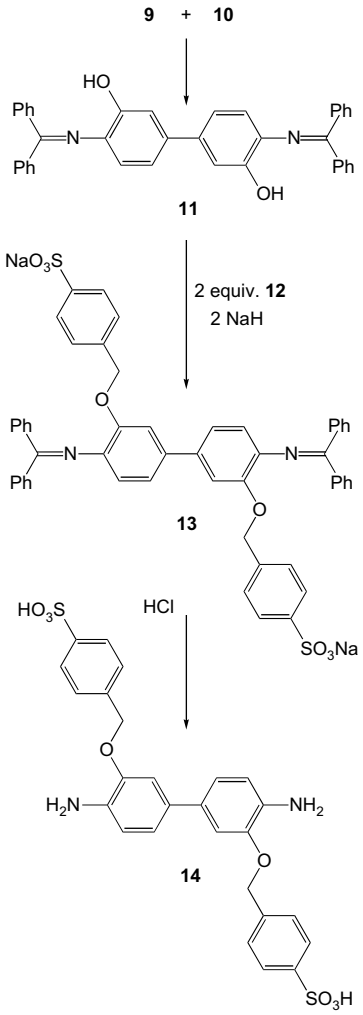

Fig. 3. Synthesis of **14**.

3.2. Polymer synthesis

Using the polycondensation reaction described by Okamoto et al. [35], a series of side chain sulfonated polyimides were synthesized as shown in Fig. 4. By adjusting molar feed ratios of sulfonated (**14**) and non-sulfonated monomers (**15**), it was possible to generate copolymers with different IEC values. Compound **15** was chosen as the non-sulfonated monomer due to the presence of an ether linkage which should afford more flexibility to the polymer main chain, thereby leading to increased hydrolytic stability and improved mechanical properties [36].

Fig. 5 shows the ^{1}H NMR spectrum of **8d**. The other polymers in the series exhibited similar spectra except that the integrals between the aromatic and aliphatic protons varied according to the composition. The aromatic protons of the side chain are located at approximately the same position found in the ^{1}H NMR spectrum of the sulfonated monomer (**14**) (7.77 and 7.49 ppm). The protons on the naphthalene units appear at 8.78 ppm. Protons at the *o*-position from the imide group (both sulfonated and non-sulfonated

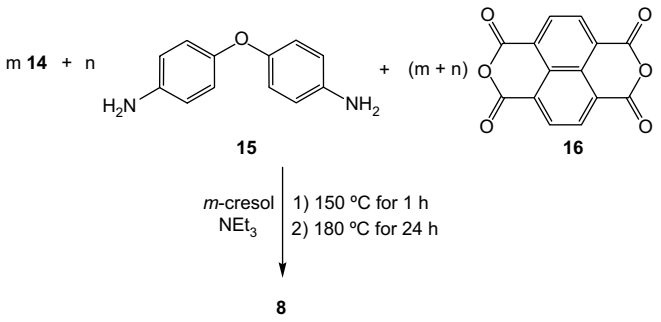

Fig. 4. Synthesis of copolymer **8**.

moieties) exhibit similar chemical shifts of 7.56 ppm. Other protons exhibit broad signals at 7.39 and 7.22 ppm. The alkyl protons with the sulfonated side chain are found at 5.28 ppm. FTIR was also used to confirm the structure. The presence of the sulfonic acid group was confirmed with peaks of S=O stretch (1123 cm^{-1}), SO_3 symmetric stretch (1037 cm^{-1}) and S–OH stretch (1012 cm^{-1}). Peaks from the imide group are also present (C=O symmetric stretch (1715 cm^{-1}), C=O asymmetric stretch (1675 cm^{-1}) and C–N stretch (1349 cm^{-1})).

The viscosity of solutions was used to provide further evidence of polymers, and an indication of polymer molecular weight by comparing the results with those in the literature [65]. Given the polyelectrolyte nature of **8**, however, the reduced and inherent viscosities increase rapidly with dilution, instead of decreasing linearly with concentration as is found for neutral polymers [66]. This phenomenon, known as the polyelectrolyte effect, is due to intramolecular and/or intermolecular ionic interactions: as the solution is diluted, the concentration of the counter ions decreases, forcing ionomer chains to extend (repulsion of anions) [67].

Attempts to mitigate the polyelectrolyte effect by the addition of 1 wt% LiCl to the DMSO solution in the form of an aqueous solution [67,68] were unsuccessful as the polymer precipitated from solution upon addition of aqueous LiCl. The reduced viscosity measured according to the method reported by Pineri et al. [69] using *m*-cresol as solvent and a triethylammonium salt as the counter ion for concentrations of 0.5 g/dL of **8d** is ~4.7 dL/g. This is in the range of the reduced viscosities for sulfonated polyimides reported in the literature (2.0–7.7 dL/g) at similar concentrations [61]. Although molecular weights cannot be extracted from this data, based on this result and that ductile thin films can be obtained by film casting from DMSO solution, it can be concluded that high molecular weight polyimides were synthesized.

4. Membrane characterization

4.1. Ion exchange capacity (IEC) and water uptake (WU) values

The ion exchange capacity of membranes as calculated independently from titration, NMR and monomer feed ratio was found to exhibit excellent agreement (±10%) amongst the different methods. The results are shown in Table 1:

As expected, WU values (Table 2) were found to increase with greater IEC values due to the increase in osmotic pressure. In contrast to sulfonated polyimides in which the sulfonic acid groups are directly attached to the backbone, copolymers **8a–f** were generally found to possess a higher WU for a similar IEC value [61]. The number of water molecule per acid group (λ) is also listed in Table 2. An important feature is that despite the increase in water content with IEC, the λ values remain relatively low and constant. This is in contrast to the vast majority of membrane types reported in the literature where λ increases with ion exchange capacity [69]. This is a positive feature since excessive swelling is a negative trait for fuel cell membranes.

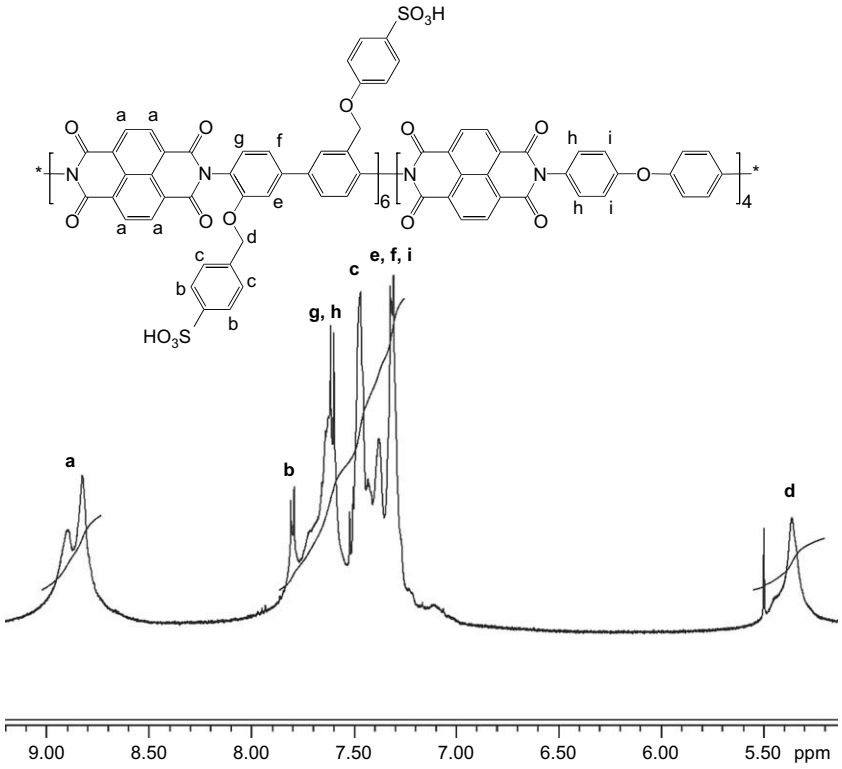

Fig. 5. ^{1}H NMR (DMSO-d_6) spectrum of **8d**.

Table 1
Ion exchange capacity (IEC) values for copolymers **8a–f**

Copolymer	Monomer feed ratio[a]	IEC (mmol/g) calculated[b]	^{1}H NMR	Titration
8a	30:70	1.10	1.12	1.03
8b	40:60	1.38	1.40	1.29
8c	50:50	1.62	1.84	1.54
8d	60:40	1.83	1.97	1.73
8e	70:30	2.02	2.14	1.94
8f	80:20	2.19	2.23	2.10

[a] Based on ratio of sulfonated monomer to unsulfonated monomer (i.e., **14**:**15**).
[b] Determined from monomer feed ratio.

4.2. Proton conductivity of copolymers *8a–f* as a function of acid and water contents

In recent publications, we presented an approach for analyzing proton conductivity data for a series of main chain, statistically sulfonated polymers [70,71]. Through this approach, it was possible to examine the effects of acid concentration [–SO_3H] and effective proton mobility (μ_{H^+}) upon conductivity (as per Eq. (10)) as well as the connections to water content. In the two studies, water content was varied by varying acid content (IEC) of the membrane[70] or relative humidity (RH) on the membrane environment [71]. In this paper, we used the first method for copolymer **8** and compared the data against results from our previous study [57] on linear sulfonated polyimides (**3**) and SPEEK (**2**), using Nafion® (**1**) as a baseline PEM. This data is summarized in Table 2 and displayed in Figs. 6–8 (see also Supplementary data).

In Fig. 6, proton conductivity values for the aforementioned PEMs are shown as a function of both acid content (IEC) and water content (λ, X_v). As has been observed for many systems, the relationship between conductivity and IEC for copolymer **8** is linear (Fig. 6a), thus suggesting that its percolation threshold has been reached by at least IEC = 1.03 meq/g. Interestingly, it appears that **8** exhibits a higher conductivity values than its linear analogue **3** as a function of acid content for IEC < 2 meq/g. Comparisons between **8** and **2**, however, are complicated by the fact that the available IEC values for the two polymer systems do not generally overlap. Nevertheless, it does appear that if samples with IEC > 2 meq/g for **2** were available, **2** would exhibit lower conductivity values than **8** whereas **2** would exhibit higher conductivity values than **8** if samples of **8** with IEC > 2.1 meq/g were available. Potential explanations for these observations can rationalized on the basis of the proton conductivity of **8** as a function of water content as well as examining the components of conductivity (i.e., μ_{H^+} and [–SO_3H]) in greater detail. Overall, however, Nafion® exhibits the highest conductivity value as a function of acid content.

As a function of water volume fraction (X_v) as seen in Fig. 6b, copolymers **3** and **8** exhibit relatively similar conductivity values and both exhibit lower values than **2**, suggesting that the polyimides make less effective use of water than **2**. More information about the effect of water content on conductivity for these polymers can be obtained by examining the relationship of conductivity to λ (Fig. 6c). However, as can be seen, the behaviour of **8** is relatively complicated in comparison to that for **2** and **3**. This is due to the fact that, although **2** appears to exhibit lower X_v values for a given IEC value (Fig. 7a) than **8**, λ values for **8** only vary within the range of 13–18 H_2O/–SO_3H over the examined IEC range (Fig. 7b) whereas **3** and **2** exhibit λ values of 15–26 and 13–42, respectively. The lack of swelling for **8** is probably due to the inherent rigidity of the polyimide backbone in comparison to **2**. Although **8** would probably exhibit higher λ values at higher IEC values, the stiff main chain would likely still prevent the greater degree of swelling as exhibited by **2**. Restricted swelling is a potential advantage in order to prevent dilution of acid sites within the polymer. However, it is interesting to note that both **3** and **8** still clearly exhibit lower conductivity values in comparison to **2** even at relatively the same λ values, thereby further suggesting that these two systems are generally unable to achieve the same conductivity values as **2** for a given water content (λ). Nevertheless, it does appear that the conductivity for **8** is higher as a factor of λ than **3**, even though the acid content (IEC) of **3** is generally higher than **8** for the available samples.

By examining how the components of proton conductivity for **8** (i.e., proton mobility and acid concentration) are related to water and acid contents, further understanding of the conductivity behaviour of **8** can be obtained. The value of proton mobility provides an assessment of how rapidly a proton is able to move through the membrane, and may be affected by the degree of proton dissociation, tethered anionic groups, degree of proton pathway tortuosity and relative proximity of neighbouring acid groups [3,70–74]. As can be seen in Fig. 8a, it appears that the mobility of **8** is greater than for **3** at IEC < 2.0 meq/g whereas only comparable, if not lower at IEC > 2.0 meq/g. It also appears that the mobility of **8** is comparable or greater than that of **2**. However, given the unavailability of higher IEC samples of **8**, it is difficult to make a direct comparison with the mobility behaviour of **2**.

By examining mobility as a function of water content (Fig. 8b and c), it is interesting to note that while generally mobility values as a function of X_v for all three systems are similar, there appears to be greater distinction between mobilities of **3** and **8** as a function of λ. This may be showing that the use of a sulfonated side chain in **8** leads to an increase in proton mobility versus the reduced mobility imparted by sulfonic acid groups being directly bonded to the main chain as in **3**. However, in spite of this, the mobility of **8** is still lower than that of **2**, suggesting that perhaps the increased mobility imparted by a side chain over a main-chain sulfonated system does not fully overcome the inherent greater rigidity of the backbone of **8** in comparison to **2**, as well as perhaps due to the relatively rigid nature of the benzyl side chain of **8**. It is interesting to note that the mobility of **8** increases at relatively fixed λ values; i.e., mobility is increasing although the amount of water available to each sulfonic

Table 2
Properties of sulfonated polyimide membranes with various IEC values

Membrane	IEC[a] (mmol/g)	WU[b] (%)	X_v[c]	λ[d]	σ[e] (S/cm)	(μ_{H^+}) (10^{-4} cm^2 s^{-1} V^{-1})	[SO_3H] (M)
8a	1.03	32	0.26	17	0.010	1.06	0.94
8b	1.29	35	0.28	15	0.017	2.10	0.86
8c	1.54	37	0.33	13	0.027	2.18	1.28
8d	1.73	40	0.37	13	0.040	2.95	1.42
8e	1.94	53	0.46	15	0.043	2.64	1.70
8f	2.10	60	0.47	18	0.060	6.00	0.97

[a] Determined from titration measurements.
[b] Water uptake.
[c] Water volume fraction.
[d] [H_2O]/[SO_3H].
[e] Measured at room temperature, samples allowed to equilibrate in H_2O prior to measurement.

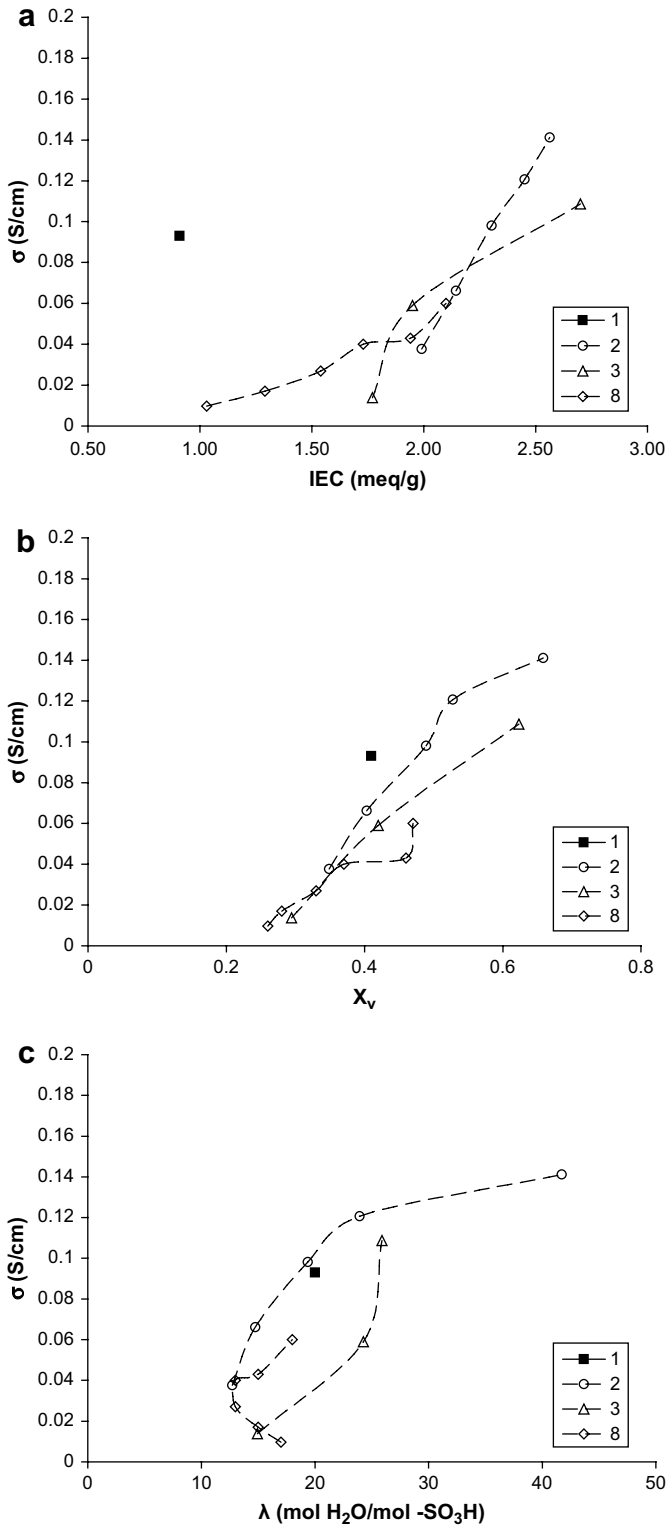

Fig. 6. Proton conductivity of **1**–**3** and **8** as a function of: (a) IEC; (b) X_v; (c) λ.

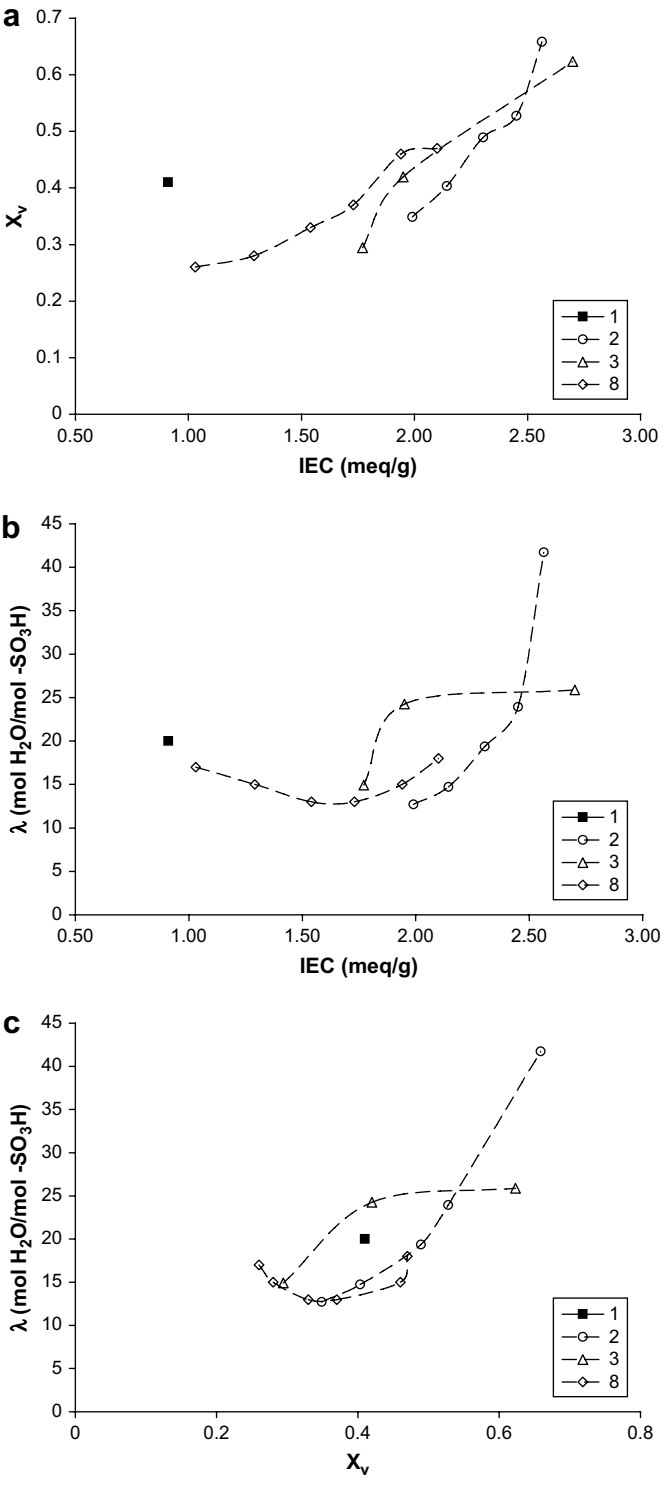

Fig. 7. Water content of **1**–**3** and **8**: (a) X_v as a function of IEC; (b) λ as a function of IEC; (c) λ as a function of X_v.

acid group is relatively unchanged. This appears to demonstrate that increasing acid content at a fixed λ value does lead to increased mobility as has been previously theorized [70–73].

Acid concentration can also be examined as a function of acid and water contents (see Table 2 and Supplementary data). The rigidity of the backbone of copolymer **8** is also evident from these plots. Whereas many polymer systems (e.g., **2**) exhibit a decrease in [–SO_3H] as a function of increasing IEC, this value is observed to generally increase for **8** and only exhibits a decrease for the sample with the highest available IEC value. This is also seen as a function of water content, particularly for [–SO_3H] versus X_v wherein at $X_v = 0.35$–0.45, acid concentration is decreasing for SPEEK whereas it is increasing for **8**.

The effective proton mobility values of **2**, **3** and **8** at infinite dilution ($X_v = 1.0$) are shown in Table 3. These were calculated in

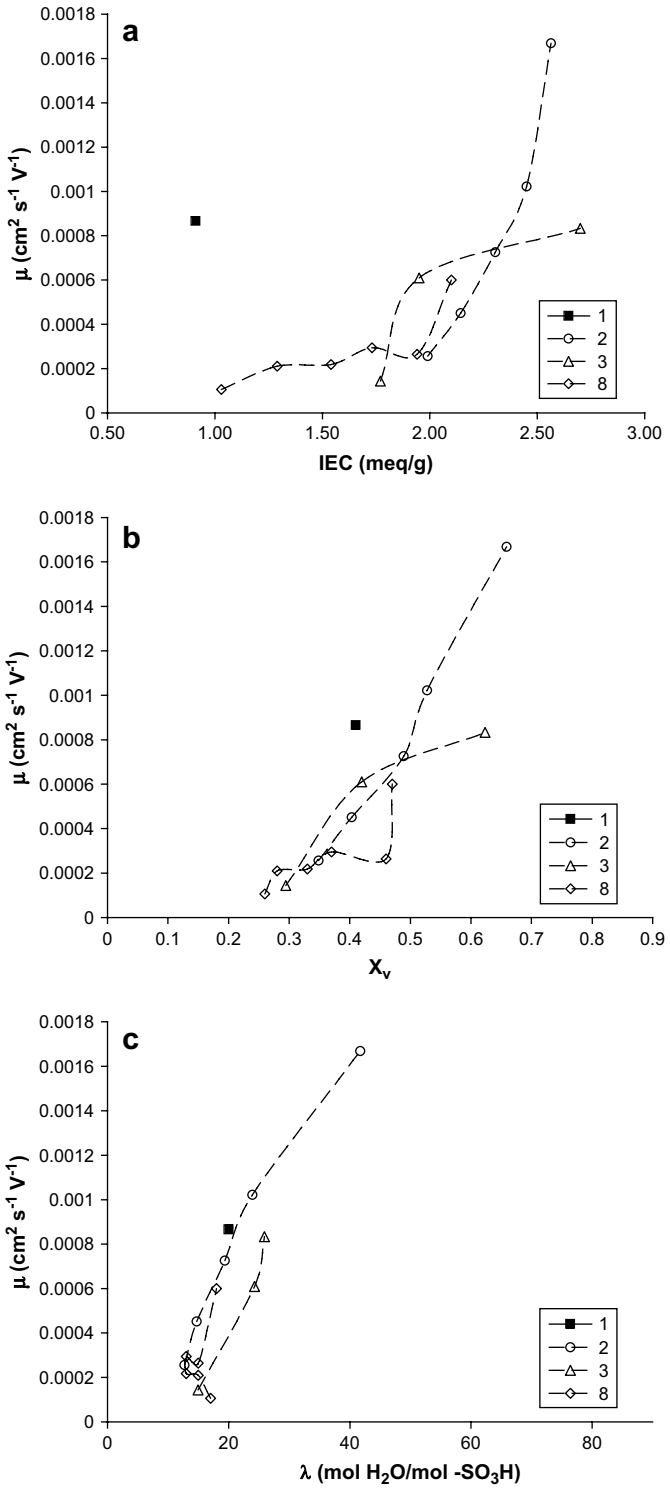

Fig. 8. Effective proton mobility of **1**–**3** and **8** as a function of: (a) IEC; (b) X_v; (c) λ.

order to remove the effects of different acid strengths for the various polymers and thereby permit comparisons between systems as well with the theoretical mobility of a free proton at infinite dilution (3.63×10^{-3} cm^2 s^{-1} V^{-1} at 25 °C) [75]. As stated in our previous work [70,71], the calculated proton mobility value for **2** at $X_v = 1.0$ is relatively consistent with that of a free proton at infinite dilution whereas the inflexible backbone of **3** significantly reduces the proton mobility. The value for copolymer **8** can be considered within standard deviation to be equivalent to that of **3**, and is likely again, at least in part, to be due to the rigid polyimide backbone restricting proton mobility. By placing the tethered sulfonate groups on side chains rather than on the main chain, it might be thought that mobility would be improved through greater potential flexibility of the side chain versus the main chain of the polymer. However, the relatively rigid nature of the benzylic side chain in **8** may prevent the achievement of any significant increase in mobility in comparison to **3**. Further work on systems with more flexible side chains may permit a more in-depth study of the potential effect of sulfonated side groups versus sulfonated main chains upon proton mobility.

Table 3
Calculated proton mobility values at infinite dilution ($X_v = 1.0$)

Polymer	μ_{H^+} at $X_v = 1.0$ (10^{-3} cm^2 s^{-1} V^{-1})	Source
2	3.2 ± 0.4	Ref. [68]
3	1.6 ± 0.7	Ref. [68]
8	1.2 ± 0.6	This work

4.3. *Membrane* ex situ *thermal and hydrolytic stabilities*

Ex situ thermal stability of the sulfonated polyimides was determined using thermal gravimetric analysis (TGA). An initial loss in mass was observed around 220 °C and has been attributed to side chain degradation and desulfonation [61], and occurs at a similar temperature to other literature examples of sulfonated polymers [50]. In the case of polymers with higher IEC values (i.e., **8b** – **f**), greater weight losses are observed. This behaviour is generally consistent with the relative amount of sulfonated moiety present in the copolymer since the degradation at 220 °C is dependent upon the amount of side chain present and acid content (IEC). The mass loss around 550 °C is likely due to thermal degradation of the polymer backbone [61].

The comparative hydrolytic stability of membranes was evaluated as the time required for the membrane, soaked in hot (80 °C) water, to substantially lose its mechanical properties. The loss of mechanical property was judged to have occurred when the membrane broke upon bending, providing a basic evaluation of the hydrolytic stability of **8** [61]. Five types of membranes were studied: N115 (**1**), **2**, **3**, **7** and **8e**. All were immersed in 80 °C water and the time required for mechanical failure determined. The results are summarized in Table 4. Copolymer **8e** remained ductile for 120 h, which was considerably longer than its linear, main-chain sulfonated analogue (**3**) which lost its mechanical integrity after less than 20 min. The angled sulfonated polyimide (**7**) retained its mechanical properties for only 120 min, but in comparison to **3**, possessed a lower IEC and was considerably thicker [54]. Given its propensity for a high degree of swelling and loss of mechanical integrity when heated in water [76,77], it is not surprising that a membrane of SPEEK (**2**) rapidly dissolves under the testing conditions. Perfluorinated **1** exhibited no observable loss in mechanical properties even after 120 h.

The enhanced hydrolytic stability for the side-chain sulfonated polyimide (**8**) versus main-chain sulfonated polyimides (**3** and **7**) is

Table 4
Hydrolytic stability at 80 °C for different membranes

Membrane	IEC (mmol/g)	Thickness (μm)	Time[a] (h)
1 (N115)	0.97	125	>120
2	2.00	103	<0.3[b]
3	2.70	85	<0.3
4	2.09	20	200[c]
7	1.80	147	2
8e	1.94	90	120

[a] Point at which polymer membrane became brittle.
[b] Dissolved in water.
[c] Ref. [49].

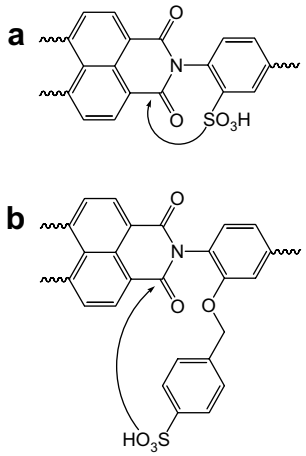

Fig. 9. Schematic representation of the proximity and basicity effects upon hydrolysis for (a) main-chain sulfonated polyimides (e.g., **3** and **7**); (b) side-chain sulfonated polyimides (e.g., **8**).

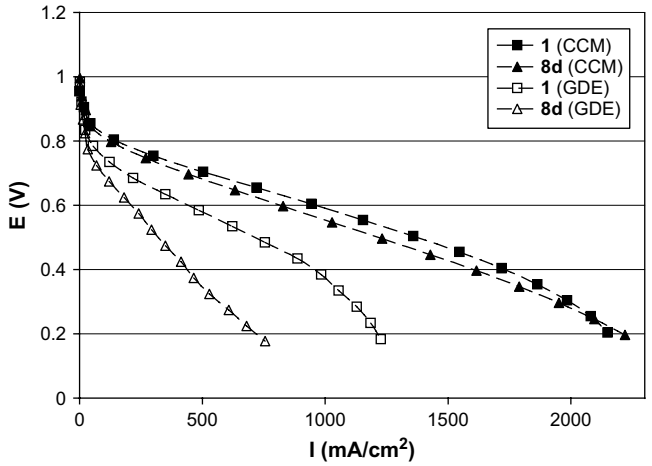

Fig. 10. Fuel cell performance for **1** and **8d** using: (a) CCM (catalyst-coated membrane)-based MEAs; (b) GDE (gas diffusion electrode)-based MEAs.

attributed to both the larger distance between the sulfonic acid and imine functionalities in the case of **8** as well as the greater strength of the basic nitrogen in **8** as compared to either **3** or **7**. This is illustrated schematically in Fig. 9. In the case of **3** and **7**, the sulfonic acid group is in close proximity to the imide functionality and thus protonation of the carbonyl group can occur more readily. For **8**, the presence of the spacer group increases the distance between the acid and imide functionalities, thereby hindering protonation. The degree of phase separation between the hydrophilic domains and the polymer backbone may also be expected to have increased by the use of spacer group [53,56] although this has yet to be confirmed. In addition to the proximity effect of the spacer group, copolymer **8** also benefits from the ether functionality and the resultant increase in basicity of the polyimide backbone. As has been demonstrated by other groups, this is known to increase the resistance of the imide functionality against hydrolysis [59,60]. It is further interesting to note that an alkyoxy-based side group appears to lead to greater hydrolytic stability (**4**) in comparison to benzylic-based side group (**8e**) at comparable acid content levels (IEC = 2.09 and 1.94 meq/g, respectively). Whether this is due to the increased flexibility of the propyloxy side chain, increased basicity (two strongly electron-donating oxygen atoms in close proximity to the imide nitrogen) or a combination thereof is not clear.

Preliminary studies of fuel cell performance of **8d** were undertaken. Two different assembling methods were used to prepare the membrane electrode assembly (MEA) as described in the experimental section: the catalyst-coated gas diffusion layer (CCGDL) and CCM (catalyst-coated membrane) techniques. Fig. 10 shows the results obtained at 50 °C. MEAs containing **8d** prepared by the CCGDL method provided only a modest fuel cell polarization curve, exhibiting 220 mA/cm^2 at 0.6 V, much lower than the Nafion®-based GDE MEA which yielded ~450 mA/cm^2 at 0.6 V. However, MEAs containing **8d** prepared by the CCM method showed a dramatic improvement in current output exhibiting ~850 mA/cm^2 at 0.6 V and similar to Nafion®-based CCGDLs which yielded ~900 mA/cm^2 at 0.6 V.

The improvement in performance of MEAs prepared by the CCM techniques has been established with other polymer systems and is due to the improvement in bonding between the catalyst layer and membrane. The CCGDL method relies on the softening of the polymer in the membrane upon hot pressing the MEAs, and its binding in the catalyst layer, which in the case of sulfonated polyimides is problematic because of its high T_g. In the case of the CCM method it is believed that the solvent in the ink serves to plasticize the polymer in the membrane so as to form a more favourable interface. These preliminary beginning of life experiments indicate that a good electrochemical interface can be obtained using the CCM method and that the membranes provide sufficient protonic and water transport under the conditions used to generate considerable current density. The stability of such MEAs is not expected to be as great as that reported for Nafion® based CCMs but further studies in this area are warranted to the extent of the degradation but such studies are not the intent of this work, which focuses on the synthesis and structure–property relationships of these polymers.

5. Conclusion

A series of novel, side-chain sulfonated polyimides (**8**) have been synthesized, characterized, and evaluated for ion exchange capacity, water uptake, volume uptake, proton conductivity, hydrolytic stability and single cell fuel cell performance. Although the hydrolytic stability of the polyimides was found to be poor, the stability of **8** was found to be an improvement over linear (**3**) and angled (**7**) sulfonated polyimides. It is surmised that this increase in stability is due to higher basicity of the amine groups as well as increased separation of the sulfonic acid group from the imide functionality. An in-depth analysis of the proton conductivity data for **8** was carried out and calculation of the value for proton mobility at infinite dilution ($X_v = 1.0$) suggests that the mobility of protons in **8** is comparable to that in **3** but significantly lower than in **2**, and likely to be indicative of the rigid polymer backbone for both **3** and **8**. Preliminary beginning of life studies on polymer **8d** incorporated within a CCM-based MEA showed similar performance as compared to a CCM-based MEA incorporating Nafion® in a fuel cell operated at 50 °C. Using the procedure outlined in this paper, future work in this area will be to synthesize derivatives of **8** containing alternative, sulfonated side groups, in order to study structure–property relationships of different side groups for this class of sulfonated polymer.

Acknowledgements

We thank the Natural Sciences and Engineering Research Council of Canada for funding. We also thank Dr. Miki Young (SFU) for running the elemental analyses, Dr. Marianne Rodgers (NRC-IFCI) for performing TGA analyses and Makoto Adachi (NRC-IFCI) for carrying out the MEA fabrication and acquiring fuel cell data.

Appendix. Supplementary data

Supplementary data associated with this article can be found in the online version, at doi:10.1016/j.polymer.2008.09.011.

References

[1] Appleby AJ, Foulkes RL. Fuel cell handbook. New York: Van Nostrand; 1989.
[2] Hickner MA, Ghassemi H, Kim YS, Einsla BR, McGrath JE. Chem Rev 2004;104(10):4587–611.
[3] Kreuer KD. J Membr Sci 2001;185(1):29–39.
[4] Savadogo O. J New Mater Electrochem Syst 1998;1:47.
[5] Savadogo O. J Power Sources 2004;127(1–2):135–61.
[6] Rikukawa M, Sanui K. Prog Polym Sci 2000;25(10):1463–502.
[7] Li Q, He R, Jensen JO, Bjerrum NJ. Chem Mater 2003;15(26):4896–915.
[8] Rozière J, Jones DJ. Annu Rev Mater Res 2003;33:503–55.
[9] Gubler L, Gürsel SA, Scherer GG. Fuel Cells 2005;3(3):317–35.
[10] Ogato N, Rikukawa M. Maxdem, Inc., US 5,403,675; 1995.
[11] Balland-Longeau A, Pereira F, Capron P, Mercier R. Commissariat à l'Energie Atomique, Fr. 0,210,008; 2002.
[12] Leninivin C. PhD Dissertation. Poitiers University; 2003.
[13] Fujimoto CH, Hickner MA, Cornelius CJ, Loy DA. Macromolecules 2005; 38(12):5010–6.
[14] Granados-Focil S, Litt MH. Abstr Papers Am Chem Soc 2003;226:U502.
[15] Granados-Focil S, Litt MH. Abstr Papers Am Chem Soc 2004;228:U657.
[16] Litt MH, Granados-Focil S, Zhang Y, Young TA. Abstr Papers Am Chem Soc 2004;228:U661.
[17] Helmer-Metzmann F, Osan F, Schneller A, Ritter H, Ledjeff K, Nolte R, et al. EP 0 574 791 A2; 1993.
[18] Wang F, Hickner M, Kim YS, Zawodzinski TA, McGrath JE. J Membr Sci 2002; 197(1–2):231–42.
[19] Ghassemi H, Ndip G, McGrath JE. Polymer 2004;45(17):5855–62.
[20] Zhang Y, Litt M, Savinell RF, Wainright JS. Polym Prepr 1999;40:480.
[21] Zhang Y, Litt M, Savinell RF, Wainright JS, Vendramint J. Polym Prepr 2000;41:1561.
[22] Faure S, Pineri M, Aldebert P, Mercier R, Sillion B. EP 897 407 A1; 1999.
[23] Cornet N, Diat O, Gebel G, Jousse F, Marsacq D, Mercier R, et al. J New Mater Electrochem Syst 2000;3:33–42.
[24] Dang TD, Bai SJ, Heberer DP, Arnold FE, Spry RJ. J Polym Sci Part B Polym Phys 1993;31(13):1941–50.
[25] Asensio JA, Borros S, Gomez-Romero P. J Polym Sci Part A Polym Chem 2002;40(21):3703–10.
[26] Jones DJ, Rozière J. J Membr Sci 2001;185(1):41–58.
[27] Peron J, Ruiz E, Jones DJ, Rozière J. J Membr Sci 2008;314(1–2):247–56.
[28] Ogawa T, Marvel CS. J Polym Sci Part A Polym Chem 1985;23(4):1231–41.
[29] Bishop MT, Karasz KE, Russo PS, Langley KH. Macromolecules 1985;18(1):86–93.
[30] Wang F, Hickner M, Ji Q, Harrison W, Mecham J, Zawodzinski TA, et al. Macromol Symp 2001;175:387.
[31] Xing P, Roberston GP, Guiver MD, Mikhailenko SD, Kaliaguine S. Macromolecules 2004;37(21):7960–7.
[32] Gao Y, Roberston GP, Guiver MD, Mikhailenko SD, Li X, Kaliaguine S. Macromolecules 2005;38(8):3237–45.
[33] Xing P, Roberston GP, Guiver MD, Mikhailenko SD, Kaliaguine S. Polymer 2005;46(10):3257–63.
[34] Schuster M, Kreuer KD, Anderson HT, Maier J. Macromolecules 2007; 40(3):598–607.
[35] Guo XX, Fang JH, Watari T, Tanaka K, Kita H, Okamoto KI. Macromolecules 2002;35(17):6707–13.
[36] Fang J, Guo X, Harada S, Watari T, Tanaka K, Kita H, et al. Macromolecules 2002;35(24):9022–8.
[37] Ghassemi H, McGrath JE, Zawodzinski TA. Polymer 2006;47(11):4132–9.
[38] Yang YS, Shi ZQ, Holdcroft S. Eur Polym J 2004;40(3):531–41.
[39] Yang YS, Shi ZQ, Holdcroft S. Macromolecules 2004;37(5):1678–81.
[40] Shi ZQ, Holdcroft S. Macromolecules 2004;37(6):2084–9.
[41] Shi ZQ, Holdcroft S. Macromolecules 2005;38(10):4193–201.
[42] Norsten TB, Guiver MD, Murphy J, Astill T, Navessin T, Holdcroft S, et al. Adv Funct Mater 2006;16(14):1814–22.
[43] Rubatat L, Shi ZQ, Diat O, Holdcroft S, Frisken BJ. Macromolecules 2006; 39(2):720–30.
[44] Ding J, Chuy C, Holdcroft S. Chem Mater 2001;13(7):2231–3.
[45] Ding JF, Chuy C, Holdcroft S. Adv Funct Mater 2002;12(5):389–94.
[46] Ding JF, Chuy C, Holdcroft S. Macromolecules 2002;35(4):1348–55.
[47] Rusanov AL. Polym Syn 1994;111:115–75.
[48] Genies C, Mercier R, Sillion S, Petiaud R, Cornet N, Gebel G, et al. Polymer 2001;42(12):5097–105.
[49] Yin Y, Fang J, Cui Y, Tanaka K, Kita H, Okamoto K. Polymer 2003;44(16): 4509–18.
[50] Yin Y, Fang J, Kita H, Okamoto K. Chem Lett 2003;32(4):328–9.
[51] Okamoto K. J Photopolym Sci Technol 2003;16(2):247–54.
[52] Yin Y, Fang JH, Watari T, Tanaka K, Kita H, Okamoto K. J Mater Chem 2004;14(6):1062–70.
[53] Yin Y, Suto Y, Sakabe T, Chen SW, Hayashi S, Mishima T, et al. Macromolecules 2006;39(3):1189–98.
[54] Yin Y, Yamada O, Suto Y, Mishima T, Tanaka K, Kita H, et al. J Polym Sci Part A Polym Chem 2005;43(8):1545–53.
[55] Miyatake K, Zhou H, Matsuo T, Uchida H, Watanabe M. Macromolecules 2004;37(13):4961–6.
[56] Yasuda T, Li Y, Miyatake K, Hirai M, Nanasawa M, Watanabe M. J Polym Sci Part A Polym Chem 2006;44(13):3995–4005.
[57] Rodgers M, Yang Y, Holdcroft S. Eur Polym J 2006;42(5):1075–85.
[58] Savard O, Yang Y, Holdcroft S. Advances in materials for proton exchange membrane fuel cell sytems. Pacific Grove, CA, U.S.A; 2005.
[59] Asano N, Aoki M, Suzuki S, Miyatake K, Uchida H, Watanabe M. J Am Chem Soc 2006;128(5):1762–9.
[60] Ohya H. Polyimide membranes. 1st ed. Amsterdam: Gordon and Breach; 1996.
[61] Yin Y, Yamada O, Tanaka K, Okamoto K. Polym J 2006;38(3):197–219.
[62] Hubbuch A, Bindewald R, Foehles J, Hanithani VK, Zahn H. Angew Chem Int Ed 1980;19(5):394–6.
[63] Hvidt T, Szarek WA, Maclean DB. Can J Chem 1988;66(4):779–82.
[64] Odonnell MJ, Boniece JM, Earp SE. Tetrahedron Lett 1978;30:2641–4.
[65] Young RJ, Lovell PA. Introduction to polymers. New York: Chapman and Hall; 1991.
[66] Debye P. J Chem Phys 1946;14(10):636–9.
[67] Gieselman MB, Reynolds JR. Macromolecules 1993;26(21):5633–42.
[68] Pals DTF, Hermans JJ. J Polym Sci 1950;5(6):733–4.
[69] Genies C, Mercier R, Sillion S, Cornet N, Gebel G, Pineri M. Polymer 2001;42(2):359–73.
[70] Peckham TJ, Schmeisser J, Rodgers M, Holdcroft S. J Mater Chem 2007; 17(30):3255–68.
[71] Peckham TJ, Schmeisser J, Holdcroft S. J Phys Chem B 2004;112(10): 4637–78.
[72] Eikerling M, Kornyshev AA. J Electroanal Chem 2001;502(1–2):1–14.
[73] Eikerling M, Kornyshev AA, Kuznetsov AM, Ulstrup J, Walbran S. J Phys Chem B 2001;105(17):3646–62.
[74] Kreuer KD, Paddison SJ, Spohr E, Schuster M. Chem Rev 2004;104(10): 4637–78.
[75] Adamson AA. A textbook of physical chemistry. New York: Academic Press, Inc; 1973. p. 506.
[76] Wu HL, Ma CCM, Li CH, Lee TM, Chen CY, Chiang CL, et al. J Membr Sci 2006;280(1–2):501–8.
[77] Mecheri B, D'Epifanio A, Di Vona ML, Traversa E, Liccocia S, Miyayama M. J Electrochem Soc 2006;153(3):A463–7.